The evolution of the sub-glacial landscape of Antarctica

Stewart S.R. Jamieson [1,2*], David E. Sugden [1] and Nicholas R.J. Hulton [1].

[1] School of GeoSciences, University of Edinburgh, Drummond St., Edinburgh, EH8 9XP. Telephone: +44 (0)131 650 2572. Fax: +44 (0)131 650 2524.

[2] Department of Geography, Durham University, Science Laboratories, South Road, Durham, DH1 3LE. Telephone: +44 (0)191 334 1800. Fax: +44 (0)191 334 1801.

[*] Corresponding author: Stewart.Jamieson@dur.ac.uk

Abstract

The aim is to investigate the evolution of the sub-glacial landscape of Antarctica using an ice-sheet and erosion model. We identify different stages of continental glaciation and model the erosion processes associated with each stage. The model links erosion to the basal thermal regime and indicates that much of the Antarctic interior may have been subject to less than 200 m of erosion. The depth of erosion reflects the presence or absence of warm-based ice and the consistency of ice flow direction. This information, linked with knowledge about landscapes of glaciation in the northern hemisphere and some simple but robust assumptions about initial topography, is used to generate a map of the subglacial Antarctic landscape in which much of the lowland interior resembles the landscapes of areal scouring typical of the Laurentian and Scandinavian shields. Near the continental margins selective linear erosion has overdeepened pre-existing river valleys by as much as 2.8 km. High elevation plateaus adjacent to such drainage systems have

survived largely unmodified under cold-based ice. High erosion rates result from steep thermal gradients in basal ice. Mountain regions such as the Gamburtsev Mountains, uplands in Dronning Maud Land and massifs in West Antarctica are likely to bear features of local alpine glaciation. Such landscapes may have been protected under cold-based ice for the last 34 Myrs or possibly longer.

1   Introduction

The aim is to investigate the pattern of glacial erosion in Antarctica with a focus on the past ca. 34 Myrs and to synthesise the history of landscape evolution through to the present day. This is important because topography determines where ice grows, flows, and erodes, as well as how glaciers respond to external forcing. Therefore better knowledge of the bed will improve predictions of ice sheet behaviour (Jamieson *et al.*, 2008; Kessler *et al.*, 2008; Oerlemans, 1984). Furthermore, This study also sets the scene for future source-to-sink investigations of sediments to the continental margin. We suggest that changes in ice thickness and flow pattern are important in determining the distribution and intensity of past and present basal processes under the Antarctic Ice Sheet.

The Antarctic landscape has been subject to erosion associated with local, regional and continental scale glacial conditions, but the nature of erosion is difficult to determine due to the inaccessibility of the bed. Glacial behaviour can be inferred from investigations of northern hemisphere glaciation and from geological evidence around the margins of Antarctica but the spatial and temporal scale of this evidence is limited (Marchant *et al.*, 1994; Rippin *et al.*, 2004; Siegert *et al.*, 2005; Taylor *et al.*, 2004). We hypothesise that

the long-term glacial landscape evolution over the entirety of Antarctica can be better understood by linking the evolution of the basal thermal regime under different stages of ice-sheet growth and decay with evidence from the beds of former northern hemisphere ice sheets. By constraining numerical models of ice and landscape development with such evidence, we present a first simulation of the geomorphic evolution of the landscape beneath the Antarctic Ice Sheet.

1.1   Antarctic Climate History

Antarctica bears the marks of pre-glacial fluvial processes operating between 118 and 34 Ma. Hydrological analysis of an isostatically compensated ice-free continent suggest the existence of dendritic river systems similar in scale to the Murray-Darling system in Australia (Jamieson *et al.*, 2005). Rivers radiated from the Gamburtsev Mountains towards the Lambert basin region of East Antarctica, Wilkes Land and the Weddell Sea basin. Pre-glacial dendritic river patterns have been identified in the Transantarctic Mountains (Baroni *et al.*, 2005; Sugden *et al.*, 1999) and in the subglacial Gamburtsev Mountains (Bo *et al.*, 2009). Fluvial denudation along the uplifted rim of the Transantarctic Mountains is of the order of 4-6 km since early rifting in the Cretaceous (Fitzgerald and Stump, 1997).

Deep-sea δ^{18}O signals are used as a proxy for changes in global glacial intensity. However, in reality they reflect a mix of global ice volume and high latitude sea surface temperature variations. Further uncertainty is inherent in the resolution of δ^{18}O data. For

example, between 34 and 14 Ma the deep-sea record does not show Croll-Milankovitch cyclicity in glacial extent despite being recorded in the geological record (Naish *et al.*, 2001), and it is smoothed so that only shifts of greater than 1 Myrs are shown. Figure 1 shows the δ^{18}O record since 34 Ma alongside 6 scenarios of ice extent which are used here as the initial basis for an analysis of broad scale conditions at the base of the Antarctic Ice Sheet. Table 1 summarises the evidence and weight we assign to each scenario during our analysis.

Although pre-Oligocene shifts in δ^{18}O indicate that small to medium-scale ice sheets may have existed earlier (Miller *et al.*, 2005), Antarctica (Fig. 2) was primed for significant ice sheet growth in the Early Oligocene by declining atmospheric CO_2 concentrations (DeConto and Pollard, 2003; Huber and Nof, 2006; Pagani *et al.*, 2005; Pearson and Palmer, 2000) and the proximity of moisture from the evolving Southern Ocean (Kennett, 1977). Pre-Oligocene coastal Antarctica was characterised by significant relief generated by fluvial erosion and topographic unloading as uplifted passive continental margins evolved (Jamieson and Sugden, 2008). High topography enabled initial ice growth at ca. 34 Ma following a sharp increase in global δ^{18}O concentrations and a rapid ca. 4 $^{\circ}$C drop in global temperature (Liu *et al.*, 2009). The dominance of locally-transported *Nothofagus* pollen assemblages (especially *Nothofagus lachlaniae*) at the Eocene-Oligocene boundary in CIROS-1 and CRP-3 cores in McMurdo Sound suggests climate at that time was similar to present-day conditions in southern Patagonia (McCulloch *et al.*, 2000; Mildenhall, 1989; Raine and Askin, 2001). Modern analogues suggest these beech species grow in mean summer temperatures of 4-12 $^{\circ}$C (Prebble *et al.*, 2006). In

Patagonia, *Nothofagus* species of low taxonomic diversity are only found close to sea level and give way to *Nothofagus* shrubs above ca. 610 m indicating marginal conditions for growth. Thus present Patagonian climate provides an envelope that can be used to infer climate in Oligocene Antarctica. Subsequently, with decreasing temperatures, vegetation survived as sparse scrub forest or as moss tundra in favoured locations (Raine and Askin, 2001). This change was recorded at 24.2-18 Ma as a transition from clay minerals like smectite, typical of forest soils, to illite indicating soil development in polar environments (Ehrmann *et al.*, 2005).

For ca. 20 Myrs following glacial inception, ice sheets may have fluctuated between near modern and almost fully deglaciated states (Miller *et al.*, 2008). Phases of warm-based glaciation produced significant meltwater deposits offshore (Marchant *et al.*, 1993; Naish *et al.*, 2001) and fluctuated on a similar scale to the Pleistocene ice sheets of the northern hemisphere. The implication is that there were inter-digitated phases of mountain glaciation, upland and regional ice caps, and full ice sheets for a period ten times longer than that experienced in the northern hemisphere during the Pleistocene. Between ca. 14.2-12.7 Ma (mid-Miocene) the climate was marked by a 6-7 °C stepped cooling in Pacific surface waters (Holbourn *et al.*, 2005; Shevenell *et al.*, 2004). This coincided with a switch from warm- to cold-based local glaciation, as recorded by changes in till facies in the McMurdo sector of the Transantarctic Mountains, reflecting a decline in atmospheric temperatures (Lewis *et al.*, 2007). The ice sheet is thought to have reached the outer edge of the continental shelf, achieving its maximum size at ca. 14 Ma, before retreating back onto land to become similar in scale to the present ice mass by ca. 13.6 Ma (Anderson, 1999; Sugden and Denton, 2004; Taylor *et al.*, 2004). Since the mid-

Miocene maximum, hyper-arid polar conditions have prevailed (Denton *et al.*, 1993; Marchant *et al.*, 1996) and the full polar ice sheet is likely to have fluctuated in size largely in response to sea level change (Denton and Hughes, 1986; Mackintosh *et al.*, 2007).

The present-day ice sheet has ice thicknesses of up to 4400 m (Fig. 2) and experiences snowfall of up to 0.5 m yr^{-1} in coastal regions with progressively drier conditions inland (Vaughan *et al.*, 1999). The mean annual air temperature at sea level is presently ca. -15 $^{\circ}$C.

1.2   Landscapes of Glaciation

Geomorphological studies show that spatial variations in basal sliding lead to distinctive glacial landscapes (Fig. 3 - Stumpf *et al.*, 2000; Sugden and John, 1976). Where ice is warm based it slides and can erode. Spectacular troughs incised into elevated plateaus are formed under conditions of selective linear erosion whereby warm-based ice flow becomes focussed, often by pre-existing topography (Fig. 3c - Jamieson *et al.*, 2008; Kessler *et al.*, 2008). Adjacent uplands often remain protected from modification beneath cold-based ice because water production and thus sliding, does not occur (Fig 3a). Landscapes generated by such thermal contrasts are most common in uplifted passive margin settings with classic examples existing around margins of Baffin Island, Greenland and the Antarctic coastline. When ice-sheet flow is less constrained, but remains warm-based it creates the landscapes of areal scouring common to the shields of North America and Europe (Fig. 3b). The degree of streamlining depends on factors such

as ice velocity and constancy of flow direction. Geomorphology thus reflects the behaviour of former ice masses and has been widely used in reconstructing mid-latitude northern hemisphere palaeo-ice-sheet dynamics (Briner *et al.*, 2006; Davis *et al.*, 2006; Hall and Glasser, 2003; Kite and Hindmarsh, 2007; Kleman *et al.*, 2007; Phillips *et al.*, 2006; Stroeven *et al.*, 2002; Sugden, 1978). We would therefore expect that Antarctica's landscape has recorded a similar set of features related to changing basal thermal and ice flow regimes.

1.3   Approach

Our approach is to investigate glacial landscape evolution patterns using a numerical ice-sheet model. The model is driven by a climate based on present day accumulation and mean annual air temperature gradients in Antarctica with transition states moving from a Patagonian, to present day Antarctic climate. The initial topography is based upon BEDMAP (Lythe *et al.*, 2001), is interpolated to 20 km resolution, and is flexurally rebounded for the removal of the present-day ice load, providing an ice-free landscape upon which to initiate glaciation. Specific objectives are:

- To reconstruct simplified scenarios of Antarctic ice extent since the Oligocene, ranging from small-scale to continental-scale ice sheets.

- To employ a model of glacial erosion coupled to an ice-sheet model to simulate the spatial distribution of landscape development under these scenarios.

- To link geomorphological understanding with model output to reconstruct how landscapes may have been modified by 34 Myrs of glaciation in Antarctica.

1.4   Ice-Sheet Model

We use the GLIMMER community ice-sheet model to simulate glacial behaviour (Rutt *et al.*, 2009).. Calculations of ice dynamics use the shallow ice approximation (Hutter, 1983) which assumes the slopes of the bedrock and of the ice surface are shallow and therefore that longitudinal stress components are negligible. The model calculates the thermodynamic field associated with ice flow on a three-dimensional grid and predicts ice rheology and the thermal regime of basal ice. Ice thickness (and therefore basal topography), heat advection and diffusion, surface air temperatures, and frictional and geothermal heating all contribute to modelled basal ice temperatures.

The geometric evolution of the modelled ice mass is influenced by patterns of ice flow, accumulation, ablation and basal melting, the latter being critical for determining the onset and distribution of glacial erosion. The model does not incorporate ice shelves but calves a percentage of its mass at the coastal ice boundary until such a stage that the East and West Antarctic Ice Sheets merge, whereupon 100% of floating ice is removed. An Earth model accounts for elastic lithospheric behaviour under adjustments in load caused by changes in ice thickness and by the removal of bedrock (Lambeck and Nakiboglu, 1980).

1.5   Erosion Model

A pre-requisite to the occurrence of erosion at the bed of an ice mass is the presence of water which allows sliding to occur (Hallet, 1979, 1996; Oerlemans, 1984; Paterson, 1994). Where pressure melting point is reached ice begins sliding and a positive feedback loop is set in motion whereby all heat from geothermal flux and frictional sliding causes further melting at the base. Modelled basal ice conditions can therefore be used to infer the distribution of selective erosion of troughs, areal scouring and, if the ice remains cold-based, the protection of the landscape.

As with earlier experiments (Jamieson *et al.*, 2008; Jamieson and Sugden, 2008), we assume constant bedrock erodibility and calculate a bulk erosion rate as a function of basal ice velocity and ice thickness. However, erosion is modelled not only as a function of ice discharge (e.g. Anderson *et al.*, 2006; Kessler *et al.*, 2008; MacGregor *et al.*, 2000; Tomkin, 2003; Tomkin and Braun, 2002), but is also directly controlled by basal thermal regime. Basal ice velocity is determined by the shear stresses generated at the base of the ice sheet, and is scaled by a parameter called basal traction (or basal slip coefficient: t_b) which controls how easily sliding can occur. The influence of basal water upon sliding patterns is incorporated whereby t_b is a parabolic function of melt-rate. This means the transition from cold to warm-based ice results in a smooth change in t_b, and thus ice velocity. This generates patterns of ice flow whereby a slippier bed results in fast basal ice flow and higher erosion rates. This proportionality holds in the case of hard-bedded systems, but is less realistic where deformable sediment drives rapid flow and mechanical friction at the bed decreases. Our model is therefore most robust across East Antarctica,

and upland parts of West Antarctica where sediment-based ice stream processes are less dominant.

1.6   Topographic and Climatic Boundary Conditions

An immediate difficulty is the circularity involved in assuming an initial topography on the basis of the glacially modified topography of today – an issue faced by all modellers investigating previous ice-sheet behaviour. However, such an approach is justified in this case because many of the large-scale topographic features pre-date the Oligocene. For example, the Transantarctic Mountains were already incised to basement rocks by the Oligocene as evidenced by the presence of eroded granite in the CIROS-1 core (Barrett, 1989; 1996). This landscape is typical of passive continental margin evolution where most uplift and incision occurs within tens of millions of years of plate separation which, in this case, occurred around 55 Myrs ago (Jamieson and Sugden, 2008). Moreover, the Gamburtsev subglacial mountains in central east Antarctica display local valley features preserved since the earliest stages of glaciation (Bo *et al.*, 2009). On a wider scale, topographic analysis shows the structure of the drainage underneath the Antarctic Ice Sheet essentially retains a pre-glacial fluvial structure. This is supported by the presence of fluvial deposits in Prydz Bay, East Antarctica which show the Lambert graben was a significant drainage outlet in the Oligocene (Cooper *et al.*, 2001).

Therefore, although the relative relief and small- to intermediate-scale features of Antarctica may have been altered by glaciation, the large-scale structures pre-date glaciation and BEDMAP is therefore robust. The main uncertainties concern parts of

West Antarctica where erosion processes have significantly affected topography around sea level since 34 Ma (Wilson and Luyendyk, 2009). However, high elevation landscapes in West Antarctica remain similar between BEDMAP and Wilson and Luyendyk's reconstruction, giving robust inception points for our study. In East Antarctica uncertainty is associated with rifted margin uplift since the Oligocene. Here the use of BEDMAP is justified because river valley spacing, which determines basal thermal regime and thus subsequent erosion of outlet glacier troughs will be largely unchanged since the Oligocene (Webb, 1994).

Currently up to 0.5 m yr^{-1} of snow falls in coastal regions of Antarctica (Fig. 4). However, accumulation rates in the interior are minimal and little surface ablation occurs due to low mean annual air temperatures at sea level of ca. -15 $^{\circ}$C (Anderson, 1999). Because the climate 34 Myrs ago was similar that of southern Patagonia today we use present-day Patagonian conditions to bracket the initiation of Antarctic ice growth in our model. The warmest mean annual air temperature that occurs in low latitude Patagonia is 7 $^{\circ}$C (McCulloch *et al.*, 2000), and we use this as the 34 Ma mean annual air temperature at sea level. We apply a uniform vertical lapse rate of -9 $^{\circ}$C km^{-1} to account for changing temperature over the land and ice surfaces.

A continental pattern of precipitation is likely to have existed ever since Antarctica separated fully from Gondwana, regardless of the presence of ice. Therefore, we use this pattern to dictate the distribution of precipitation throughout our experiment. Mean annual precipitation near the margins of the present-day southern Patagonian ice fields is ca. 2 m yr^{-1} (McCulloch *et al.*, 2000). We use this value to uniformly scale the present-

day pattern of Antarctic accumulation, increasing it by four times at the coast to a maximum value of 2 m yr^{-1}.

In order to model scenarios of ice extent between glacial inception and a full-scale ice sheet, we start with a mean annual air temperature at sea level of 7 $^{\circ}$C and mean annual precipitation of 2 m per year. During the experiment we reduce temperature in 1 $^{\circ}$C steps every 50 kyrs until it reaches the present-day value of -15 $^{\circ}$C. Precipitation is reduced linearly from 2 m per year to 0.5 m per year. This configuration allows ice sheets to reach equilibrium with climate at each stage. Finally, we let the final continental-scale ice-sheet reach full equilibrium with its climate for a further 50 kyrs.

We model ablation using a positive degree day scheme (Reeh, 1991). This assumes melt at the ice surface is proportional to the number of days that air temperature (T) is above freezing. The number of positive degree days is therefore proportional to the energy available for melting. Melt (w) is calculated by:

$$w = \alpha \int_{year} \max(T,0)dt \qquad\qquad (5.1)$$

where α is the degree day factor describing the density and albedo of snow or ice. The melt calculation applies an annual sinusoidal cycle to air temperature to represent seasonality and is generated using mean annual temperature and a measure of its variability. Diurnal departures from the sinusoidal temperature regime are accounted for by assuming any variability has a normal distribution with a standard deviation of 5 $^{\circ}$C. Finally, a firn model accounts for the fraction of melted snow that refreezes to become

superimposed ice. Profile X-Y shows the accumulation and ablation pattern generated by this scheme (Fig. 4).

1.7   Sensitivity Testing

To test the capability of the model to generate realistic ice-sheet geometries we use present-day climatic data to model the current Antarctic Ice Sheet and compare the output with the present-day ice surface (Fig. 5). The model over-estimates inland ice thicknesses by less than 500 m on average and a lack of ice-shelf model results in ice grounding further into the Ross Sea than is actually the case. Most importantly however, patterns of basal sliding generate streaming ice and zones of erosion that resemble those of the balance velocity map of Antarctica (Bamber *et al.*, 2000; Huybrechts *et al.*, 2000). The good match suggests the model is successful and thus can be usefully applied to past ice sheets of varying size.

Model sensitivity to precipitation rates was also tested. As McCulloch et al. (2000) indicate, precipitation in localised parts of Patagonia reaches 3 m yr^{-1}. Therefore a sensitivity experiment uses this higher figure of 3 m of precipitation at the first stage of ice-sheet growth and, as before, linearly reduced this amount to the present-day Antarctic maximum. Glacier extent and landscape evolution are essentially similar to our first model, though ice builds up more rapidly.

2   Experiments

2.1   **Glacier Extent and Erosion**

Modelling a full 34 Myrs of glacial behaviour in a dynamic way is not yet computationally feasible. It is therefore helpful to focus on six scenarios of ice extent and associated erosion rates in Antarctica (Fig. 6). These scenarios are chosen as being representative of an envelope of possible ice-sheet extents since the Oligocene (Fig. 1). They are not intended to relate precisely to rapid recorded changes in ice extent, but rather to a mix of scales that will allow the average basal conditions over each time period to be analysed. The error associated with this is difficult to determine precisely. For example, if the ice sheet fluctuated over Croll-Milankovitch timescales between 34 and 14 Ma, there would be little advantage in analysing a single average ice extent scenario because it would not encompass the full range of possibilities. Therefore we use scenarios a-c (Fig. 1) in order to encompass the range of basal conditions that relate to this period. Thus, despite inherent error relating to spatio-temporal ice mass behaviour, our experiments will still capture key changes in the patterns of long-term, large-scale landscape evolution.

Scenario A

Under initial Patagonian conditions (Fig. 6a), glaciation is restricted to local ice caps over uplands in Dronning Maud Land, the Gamburtsev Mountains and in the Ross sector of the Transantarctic Mountains. Numerous smaller glaciers also grow across MacRobertson Land adjacent to the Lambert Graben region. Ice in West Antarctica is limited to local

mountain glaciers and ice caps in upland areas. In this scenario erosion occurs around the fringes of the ice masses, especially in the vicinity of the equilibrium line altitude (ELA) and below. The central core of the Gamburtsev Mountains is covered by cold-based ice.

Scenario B

Under cooler and drier conditions, regional-scale ice masses form over the Gamburtsev and Dronning Maud areas (Fig. 6b). The drop in temperature of ca. 4 °C produces ice masses up to ca. 3000 m thick as accumulation centres merge. The ice margin on the eastern fringe of the Gamburtsev region lies on the shore of present-day Lake Vostok. Ice remains restricted to the Transantarctic Mountains and to mountain massifs in West Antarctica. Zones of warm-based ice extend down into the lowlands of East Antarctica. and stream towards Enderby Land. Under the two larger ice masses, significant portions of the bed experience widespread but low rates of erosion. Cold-based ice covers significant areas of upland Dronning Maud Land and the Gamburtsev Mountains.

Scenario C

A further drop in temperature of 1.6 °C brings mean annual air temperatures at sea level close to zero. Most local and regional ice masses coalesce to form a single ice sheet but it is not connected to ice centres in the Transantarctic Mountains (Fig. 6c). It is likely that significant volumes of melt water flow to the ice-free area separating the two. The lowland landscape surrounding the Gamburtsev Mountains is covered by erosive warm-based ice but the mountain core remains beneath cold-based ice.

Scenario D

As the mean annual air temperature at sea level drops to ca. -4 $^{\circ}$C, the East Antarctic Ice Sheet amalgamates with regional ice in the Transantarctic Mountains creating a continental-scale ice-sheet and massive ice discharge through the Transantarctic Mountains (Fig. 6d). The majority of the East Antarctic Ice Sheet margin discharges directly into the ocean, as does a secondary ice sheet in central Wilkes Land and most West Antarctic ice. Basal ice temperatures around the ice-sheet margin increase and individual troughs channel rapid ice flow. Zones of cold-based ice around the East Antarctic mountain cores expand.

Scenario E

With sea level temperatures at -6.6°C the full East Antarctic Ice Sheet expands and ice covers all land above sea level in West Antarctica (Fig 6e). Around the George V Coast and Wilkes Land ice extent is restricted due to the simplicity of our calving assumptions. Although the pattern of erosion changes little between scenarios *D* and *E*, it shows a key change in that erosion along the Antarctic Peninsula becomes selective as cold-based ice envelopes the high plateaus.

Scenario F

The establishment of a West Antarctic Ice Sheet similar to the present-day heralds the final full polar ice-sheet (Fig. 6f). This occurs when mean annual air temperature at sea level is lowered to ca. -12 $^{\circ}$C. The glacial configuration remains the same as temperatures decline further to -15 $^{\circ}$C, partly as a result of the lack of an ice-shelf model in our approach. Nonetheless, the model simulates the main changes in basal conditions that

would leave their mark upon the Antarctic landscape. Because ice thicknesses in East Antarctica increase under this scenario, a zone of warm-based ice between the Transantarctic Mountains and the Lambert region is established. Under a full West Antarctic Ice Sheet, gradients between zero and the maximum erosion rate of 0.2 mm yr^{-1} are steep.

2.2   Thermal Regime and Glacial Landscape Evolution

Understanding the relationship between former ice masses and the landscape in the northern hemisphere helps link modelled basal thermal regime to a range of possible glacial landscapes (Fig. 3). Where the ice sheet flows across the upland rim of much of East Antarctica the basal thermal regime alternates between warm- and cold-based ice. Such conditions are likely to form a fjord landscape akin to that of the coasts of Labrador or East Greenland (Fig. 3c). Trough overdeepening occurs as warm-based ice is funnelled down existing valley systems whereas adjacent upland plateaus survive with little or no erosion under cold-based ice. Advection of heat flow in this situation reinforces the thermal and erosional contrast because heat is preferentially drawn from the uplands and into the thicker faster-flowing ice occupying the valleys. The relationship of erosion to ice flux means that overdeepening will be enhanced in areas of rapid flow and convergence, especially where ice flow directions remain stable. Where cold-based ice is extensive, larger upland plateau regions, such as those in the eastern Scottish Highlands, the mountainous axis of northern Scandinavia, or the Arctic Canadian archipelago, are protected from erosion (Fig. 3a). In contrast, where ice is warm-based, as is common in

lowlands, the landsurface will be subjected to areal scouring with wide regions becoming sculpted into a landscape of bedrock knobs and hollows (Fig 3b). The sliding velocity of the ice and its directional stability is important. The landscape will be smoothed and streamlined under fast and constant ice flow directions as for example in the ice stream hinterlands, but will become more complex if subjected to changes in ice direction during glacial cycles.

In order to illustrate this latter point, Figure 7 shows the *maximum* change in basal ice flow directions between scenarios *A-F*. Approximately 50 % of the Antarctic bed has been subjected to warm-based ice experiencing minor changes in direction of basal flow, whether influenced by local, regional or continental ice. The implication is that in these areas, ice will have eroded smooth and linear landforms at the bed (Fig. 7a). Around 35 % of the East Antarctic bed has seen changes in basal flow direction of between 10° and 45° (Fig. 7b), with the remainder changing by more than 45°. Under these latter conditions, scoured topography is likely to be irregular, displaying a superimposed patchwork of erosional features reflecting ice flow in different directions. Contrasts between constant and varying basal flow directions are strongest in Dronning Maud Land and the Transantarctic Mountains. Here, the inland flanks of upland areas will have landforms reflecting regional flow inland overprinted by continental ice-sheet flow in the opposite direction. Their coastal regions are characterised by troughs resulting from directionally constant linear incision beneath both local and continental ice. Such a scenario mirrors that of the Scandinavian Peninsula. The Swedish ribbon lakes bear evidence of flow from a regional ice-sheet centred on the Scandinavian upland axis which has subsequently been overprinted by continental ice flowing in the opposite direction

from the Baltic basin. The Norwegian flank has constant westward ice flow under both regional and continental ice-sheets (Kleman *et al.*, 2007).

2.3   Linking Patterns of Erosion to Antarctic Chronology

A clearer understanding of the landscape evolution experienced over 34 Myrs can be gained by linking the chronology of changes in past climate to our 6 model scenarios. By doing this, we can make end-member calculations of the volume of erosion, and can identify the lengths of time over which warm-based and cold-based ice might have been present in a location.

To achieve this we calculate how long each scenario of ice-sheet extent might have existed according to geological evidence (Table 1; Fig.1). We then integrate erosion patterns under each of the 6 scenarios accounting for the average time spent at or between each scenario. Because of uncertainties about the lithological susceptibility of the Antarctic bed to glacial erosion, the model output is scaled to assume a maximum erosion rate and then time-integrated to calculate the amount of material removed. There are 3 separate integrations scaling modelled erosion to 0.1 mm yr^{-1}, 0.2 mm yr^{-1} or 0.5 mm yr^{-1}. The highest rate is based on Rocchi et al's (2006) calculation from Dorrel Rock of 3000 m in the 6 Myrs from 34-28 Ma, an upper limit of erosion likely to occur over extended periods of time on bedrock surfaces under a warm-based glacial regime.

The pattern of erosion is the same in each integration (Fig 8a), but the magnitude of excavation differs. Using the intermediate value for maximum erosion rate (0.2 mm yr^{-1}), up to ca. 2800 m of excavation can be achieved if topographic focussing of erosion is

particularly strong, but this is rare. Much of the interior land surface has been subject to less than 200 m of erosion. This is in-line with rates across northern hemisphere shields where tens of meters of material was eroded during the Quaternary (Kleman *et al.*, 2007). Excavation near the coast increases as expected given a) the long-term existence (>12-14 Myrs) of the continental scale ice mass and an ELA close to the coast, b) the larger volumes of ice that are discharged under continental ice conditions, and c) isostatic feedback whereby rock uplift compensates for, and thus partially replenishes, material for erosion (Jamieson *et al.*, 2008; Kerr, 1993).

Sensitivity tests show that by varying the maximum erosion rates used in the integrations to between 0.5 mm yr^{-1} and 0.1 mm yr^{-1}, the greatest depths of excavation range from ca. 7000 m to ca. 1400 m respectively. The former is unlikely because there are no present-day troughs that approach this depth and because volumes of material sequestered offshore are less than required. For each of the three maximum erosion rates tested, overall volumes of sediment removed would be: 0.5 x 10^6 km^3, 1.004 x 10^6 km^3 and 2.51 x 10^6 km^3 respectively. These convert to spatially averaged erosion rates (including areas of cold-based ice) of 0.0011, 0.0022 and 0.0055 mm yr^{-1}. The lower two of these calculations compares quite well with estimates of glacigenic sediment volume from Prydz Bay where it is estimated that over the past 12-14 Myrs, average erosion rates were between 0.001-0.002 mm yr^{-1} (Cooper *et al.*, 2001; Cooper *et al.*, 1991; Jamieson *et al.*, 2005; O'Brien *et al.*, 2001; Stagg, 1985). Therefore, the intermediate integration, which corresponds to a maximum erosion rate of 0.2 mm yr^{-1}, may be a reasonable first estimate.

It is possible that a large ice sheet grew as cooling occurred at the Eocene-Oligocene transition (Barrett, 1989). We did not include this in our analysis, but if correct, our erosion estimates would need to be increased by up to ca. 200 m in the peripheral troughs if the expanded ice existed, as is suggested, for a further 0.4 Myrs before decreasing in scale (Zachos and Kump, 2005). Over inland Antarctica however, this figure would be significantly smaller (low tens of metres). If full ice sheets persisted for longer than the timescales employed in our analysis, then the implication is that our erosion estimates are a minimum.

Further analysis makes it possible to distinguish between different modes of basal process (selective, areal, protective). This is important because the stability of these processes, particularly under conditions of areal scour, will control the roughness of the landscape. The distinction between selective erosion and areal scour is driven largely by local relief in that selective erosion is focussed in pre-existing valleys and cold-based ice covers adjacent uplands. We assume selective erosion occurs where erosion rates are in the top 60% of the modelled range. Areal scour is assumed in the lower 40% of the range. Protection is defined where erosion rate is zero at any time step. This classification is sensitive to the ratio but by using a 60/40 split, maximum erosion correlates strongly with large troughs where we know erosion is typically selective. Our assessments are then time-integrated to reflect the duration of each mode of erosion.

Figure 8b shows selective erosion occurs for at least 12 Myrs where flow is stable. Indeed a few localities, such as the Queen Maud Mountains, the Lambert Graben feeder glaciers and Princess Ragnhild Coast, experienced selective erosion for 20-34 Myrs. Figure 8c indicates areal scour has been widespread, and is often established for over 20 Myrs. In

particular, our model suggests that parts of Queen Maud Land have been undergoing scouring since the Oligocene. Conversely, a number of areas of the East Antarctic bed may have been subject to little or no erosion since the Oligocene (Fig. 8d). The pre-glacial landscapes of the Gamburtsev Mountains, large sections of Dronning Maud Land and parts of the inner Transantarctic Mountains are expected to have experienced long periods when they were preserved beneath cold-based ice.

Figure 9 links the evolution of modelled basal thermal regime (Fig. 8b-d) and basal ice flow direction (Fig. 7) to predict the geomorphological nature of the present-day subglacial landscape. The key features of this map are that: 1) the inner mountain cores are preserved, probably as an alpine landscape; 2) the innermost flanks of the uplifted margins of East Antarctica have been subject to changing ice flow direction and are thus likely to be less well streamlined; 3) the majority of the bed of the West Antarctic Ice Sheet has been modified by ice flowing in a constant direction, producing streamlined bedrock features in the ice stream hinterlands; 4) portions of the lowland interior between the Gamburtsev Mountains and the coastal ranges are subject to large-scale changes in ice flow direction, generating irregular bedrock landscapes; 5) upland areas, especially near the coast, are landscapes of selective linear erosion.

3   *Discussion*

Erosion by local glaciers is generated by our model in a number of areas prior to being protected under cold-based ice. Our results are supported by a recent remote sensing study of the Gamburtsev Mountains showing features typical of local mountain glaciation

under warm-based glacial conditions, creating U-shaped valleys, overdeepenings and corries (Bo *et al.*, 2009). The Gamburtsevs have since experienced little or no erosion due to the presence of cold-based ice for at least 34 Myrs. In Dronning-Maud Land cirques and U-shaped valleys have been preserved for at least 2.5 Myrs (Holmlund and Näslund, 1994), and our model suggests that their age could be much older. Our results are also consistent with the survival of an alpine landscape with a tillite deposited by local warm-based ice around the Ricker Hills in the Victoria Land sector of the Transantarctic Mountains (Baroni *et al.*, 2008). Furthermore, if local or regional-scale ice sheets existed prior to 34 Ma (Matthews and Poore, 1980; Miller *et al.*, 2005), the age of some landscapes surviving under long-lived cold-based ice could be significantly older than 34 Myrs.

Our model, and field evidence from the Prince Charles Mountains (Hambrey *et al.*, 2007) indicates that selective erosion under continental scale ice has exaggerated relief along pre-glacial fluvial systems, causing overdeepening in valleys whilst preserving adjacent upland surfaces. Sediments that make up the Late-Miocene Pagodroma Group have survived on uplands relatively untouched by glaciation at the same time as erosion occurred in the neighbouring Lambert trough and its tributaries.

A similar juxtaposition of preservational and erosional landforms has been found from field observations in the Transantarctic Mountains, Marie Byrd Land, around the rim of Dronning Maud Land and along the Antarctic Peninsula (Baroni *et al.*, 2005; Naslund, 2001; Sugden and Denton, 2004; Sugden *et al.*, 2005). The large-scale form of the pre-glacial landscape therefore remains preserved, although in areas of selective flow the amplitude of this landscape may be enhanced through both erosion and adjacent uplift

(Jamieson *et al.*, 2008; Stern *et al.*, 2005). Formerly glaciated parts of the northern hemisphere conform to this pattern (Goodfellow *et al.*, 2007; Kleman *et al.*, 2007; Sugden, 1978). Such landscapes reflect a stability that is promoted by thermal feedback driven by streaming of ice through narrow topographic features (Jamieson *et al.*, 2008). This causes heat to be drawn towards troughs, and the steep, confining topography means that the thermal gradient is sharp and that heat cannot escape from the fast-flowing ice. Thus areas laterally adjacent to regions of selective flow can remain relatively cold, enabling plateaus to be protected whilst reinforcing the contrast in ice temperature. Therefore if ice is now flowing and eroding selectively, it is likely to have done so under previous eposides of glaciation.

In contrast, smoother areas of the landscape tend to experience areal scouring. Confirmation that landscapes of areal scouring are likely to be widespread in Antarctica is provided in regions previously covered by ice during expanded glaciation at 14 Ma. Warm-based ice existed across the continental shelf where scoured surfaces dip towards the land (Anderson, 1991; Anderson and Bartek, 1992) and in parts of the inner shelf of the Antarctic Peninsula where sediment cover has been removed (Anderson, 1999). Moreover, Denton and Sugden (2005) describe such scoured landscapes extending from sea level to 2100 m in elevation at the front of the Transantarctic Mountains in the Ross Sea sector that are associated with areal scouring under more expansive ice conditions.

4   Conclusions

This paper tests a new basis for interpreting the bedrock landscape underneath the Antarctic Ice Sheet following its evolution under local, regional and continental scales of glaciation over the last 34 Myrs. By comparing modelled erosion patterns to geological data from Antarctica and using constraints established in the northern hemisphere we argue that the geometry of both the ice mass and the pre-glacial landscape influence processes of glacial erosion in a predictable way (Fig. 9). The main outcomes of this work are:

- Our simple model approach provides an insight into changing ice-sheet extent, basal thermal regimes, and glacial landscape evolution in Antarctica. Between 34 − 14 Ma there are cyclic fluctuations between local, regional and continental ice-sheet extent that have been superimposed upon a progressive cooling of climate. Maximum ice-sheet extent is reached at 14-13.6 Ma. Since 13.6 Ma the ice sheet has been similar in scale to that of the present-day.

- A wave of erosion (largely areal scour in the vicinity of the ELA) sweeps across the continent with every ice-sheet expansion. At the uplifted and dissected topography near the coast, focussed flow and selective erosion develops, overdeepening the radial pre-existing fluvial valley systems.

- Upland glacial inception points in central Antarctica and Dronning Maud Land were initially eroded by local glaciers. These early landscapes have survived under cold-based ice and may date to before the Early Oligocene.

- Since the Oligocene, much of the Antarctic interior probably experienced less than 200 m of erosion, while some coastal troughs were excavated by up to 2800 m. Low erosion rates over much of the continental interior are consistent with estimates of erosion beneath northern hemisphere ice sheets.

- The relative stability of erosion patterns under warm-based ice allows bed roughness to be anticipated. Where ice flow directions remain constant the landscape is likely to be streamlined. Where ice flow direction has changed the landscape will be an irregular palimpsest of superimposed morphologies.

- The model of erosion provides the basis for calculating sediment transport routes and lithological provenance. This study sets the scene for a future source-to-sink assessment of landscape evolution and will help extend a recent reconstruction of the Oligocene landscape of West Antarctica (Wilson and Luyendyk, 2009) to the whole of the continent.

References:

Anderson J. 1991. The Antarctic continental shelf: results from marine geological and geophysical investigations. In: Tingey RJ (Ed), *The Geology of Antarctica*. Clarendon Press, Oxford, pp. 285-334.

Anderson J, Bartek LR. 1992. Cenozoic glacial history of the Ross Sea revealed by intermediate resolution seismic reflection data combined with drill site information. In: Kennett JP and Warnke DA (Eds), *The Antarctic Paleoenvironment: A perspective on Global Change I.* Antarctic Research Series. American Geophysical Union, Washington D.C., pp. 231-263.

Anderson JB. 1999. *Antarctic Marine Geology*. Cambridge University Press, Cambridge, 289 pp.

Anderson RS, Molnar P, Kessler MA. 2006. Features of glacial valley profiles simply explained. *Journal of Geophysical Research*, **111**(F1): F01004 doi: 10.1029/2005JF000344.

Bamber JL, Vaughan DG, Joughin I. 2000. Widespread complex flow in the interior of the Antarctic ice sheet. *Science*, **287**(5456): 1248-1250.

Baroni C, Fasano F, Giorgetti G, Salvatore MC, Ribecai C. 2008. The Ricker Hills Tillite provides evidence of Oligocene warm-based glaciation in Victoria Land, Antarctica. *Global and Planetary Change*, **60**: 457-470.

Baroni C, Noti V, Ciccacci S, Righini G, Salvatore MC. 2005. Fluvial origin of the valley system in northern Victoria Land (Antarctica) from quantitative geomorphic analysis. *Bulletin of the Geological Society of America*, **117**(1-2): 212.

Barrett PJ (Ed). 1989. *Antarctic Cenozoic history from the CIROS-1 drill-hole, McMurdo Sound, Antarctica.* NZDSIR Bulletin, 245 pp.

Barrett PJ. 1996. Antarctic palaeoenvironment through Cenozoic times - a review. *Terra Antarctica*, **3**: 103-119.

Bo S, Siegert MJ, Mudd S, Sugden D, Fujita S, Xiangbin C, Yunyun J, Xueyuan T, Yuansheng L. 2009. The Gamburtsev mountains and the origin and early evolution of the Antarctic Ice Sheet. *Nature*, **459**: 690-693.

Briner JP, Miller GH, Davis PT, Finkel RC. 2006. Cosmogenic radionuclides from fiord landscapes support differential erosion by overriding ice sheets. *Geological Society of America Bulletin*, **118**(3-4): 406-420.

Cooper AK, O'Brien PE, Party LSS. 2001. Early stages of East Antarctic glaciation - insights from drilling and seismic reflection data in the Prydz Bay region. In: Florindo F and Cooper AK (Eds), *The Geologic Record of the Antarctic Ice Sheet from Drilling, Coring and Seismic Studies, Extended abstracts.* Quaderna di Geofisca, pp. 41-42.

Cooper AK, Stagg H, Geist E. 1991. Seismic stratigraphy and structure of Prydz Bay, Antarctica: implications from ODP Leg 119 drilling. In: Barron JB and Larsen B (Eds), *Ocean Drilling Program Leg 119, Scientific results.*, College Station, Texas, pp. 5-25.

Davis PT, Briner JP, Coulthard RD, Finkel RW, Miller GH. 2006. Preservation of Arctic landscapes overridden by cold-based ice sheets. *Quaternary Research*, **65**(1): 156-163.

DeConto RM, Pollard D. 2003. Rapid Cenozoic glaciation of Antarctica induced by declining atmospheric CO_2. *Nature*, **421**(6920): 245-249.

Denton GH, Hughes TJ. 1986. Global Ice-Sheet System Interlocked by Sea-Level. *Quaternary Research*, **26**(1): 3-26.

Denton GH, Sugden DE. 2005. Meltwater features that suggest Miocene ice-sheet overriding of the Transantarctic Mountains in Victoria Land, Antarctica. *Geografiska Annaler*, **87 (A)**(1): 67-85.

Denton GH, Wilch TI, Sugden DE, Marchant DR, Hall BL. 1993. East Antarctic ice sheet sensitivity to Pliocene climatic change from a dry valleys perspective. *Geografiska Annaler, Series A 75*, **A**(4): 155-204.

Ehrmann W, Setti M, Marinoni L. 2005. Clay minerals in Cenozoic sediments off Cape Roberts (McMurdo Sound, Antarctica) reveal palaeoclimatic history. *Palaeogeography Palaeoclimatology Palaeoecology*, **229**(3): 187-211.

Fitzgerald PG, Stump E. 1997. Cretaceous and Cenozoic episodic denudation of the Transantarctic Mountains, Antarctica: New constraints from apatite fission track thermochronology in the Scott Glacier region. *Journal of Geophysical Research-Solid Earth*, **102**(B4): 7747-7765.

Goodfellow BW, Stroeven AP, Hättestrand C, Kleman J, Jansson KN. 2007. Deciphering a non-glacial/glacial landscape mosaic in the northern Swedish mountains. *Geomorphology*, **93**: 213-232.

Gordon J. 1981. Ice-scoured topography and its relationship to bedrock structure and ice movement in parts of northern Scotland and West Greenland. *Geografiska Annaler*, **63A**: 55-65.

Hall AM, Glasser NF. 2003. Reconstructing the basal thermal regime of an ice stream in a landscape of selective linear erosion: Glen Avon, Cairngorm Mountains, Scotland. *Boreas*, **32**(1): 191-207.

Hallet B. 1979. A theoretical model of glacial abrasion. *Journal of Glaciology*, **23**(89): 39-50.

Hallet B. 1996. Glacial quarrying: A simple theoretical model. *Annals of Glaciology*, **22**: 1-8.

Hambrey MJ, Glasser NF, McKelvey BC, Sugden DE, Fink D. 2007. Cenozoic landscape evolution of an East Antarctic oasis (Radok Lake area, northern Prince Charles Mountains), and its implications for the glacial and climatic history of Antarctica. *Quaternary Science Reviews*, **26**(5-6): 598-626.

Holbourn A, Kuhnt W, Schulz M, Erlenkeuser H. 2005. Impacts of orbital forcing and atmospheric carbon dioxide on Miocene ice-sheet expansion. *Nature*, **438**(7067): 483-487.

Holmlund P, Näslund JO. 1994. The glacially sculptured landscape in Dronning-Maud Land, Antarctica, formed by wet-based mountain-glaciation and not by the present ice-sheet. *Boreas*, **23**(2): 139-148.

Huber M, Nof D. 2006. The ocean circulation in the Southern Hemisphere and its climatic impacts in the Eocene. *Palaeogeography Palaeoclimatology Palaeoecology*, **231**: 9-28.

Hutter K. 1983. *Theoretical Glaciology. Mathematical Approaches to Geophysics*. D.Reidel Publishing Company, Boston, Lancaster.

Huybrechts P, Steinhage D, Wilhelms F, Bamber J. 2000. Balance velocities and measured properties of the Antarctic ice sheet from a new compilation of gridded data for modelling. *Annals of Glaciology*, **30**: 52-60.

Jamieson SSR, Hulton NRJ, Hagdorn M. 2008. Modelling landscape evolution under ice sheets. *Geomorphology*, **97**(1-2): 91-108.

Jamieson SSR, Hulton NRJ, Sugden DE, Payne AJ, Taylor J. 2005. Cenozoic landscape evolution of the Lambert basin, East Antarctica: the relative role of rivers and ice sheets. *Global and Planetary Change*, **45**(1-3): 35-49.

Jamieson SSR, Sugden DE. 2008. Landscape evolution of Antarctica. In: Cooper AK et al. (Eds), *Antarctica: A Keystone in a Changing World - Proceedings of the 10th International Symposium on Antarctic Earth Sciences*. The National Academies Press, Washington D.C., pp. 39-54.

Kennett JP. 1977. Cenozoic evolution of Antarctic glaciation, the circum-Antarctic Ocean and their impact on global palaeoceanography. *Journal of Geophysical Research*, **82**: 3843-3860.

Kerr A. 1993. Topography, climate and ice masses: a review. *Terra Nova*, **5**(4): 332-342.

Kessler MA, Anderson RS, Briner JP. 2008. Fjord insertion into continental margins driven by topographic steering of ice. *Nature Geoscience*, **1**(6): 365-369.

Kite ES, Hindmarsh RCA. 2007. Did ice streams shape the largest channels on Mars? *Geophysical Research Letters*, **34**(19).

Kleman J, Stroeven AP, Lundqvist J. 2007. Patterns of Quaternary ice sheet erosion and deposition in Fennoscandia and a theoretical framework for explanation. *Geomorphology*, **doi: 10.1016/j.geomorph.2007.02.049**.

Lambeck K, Nakiboglu SM. 1980. Seamount loading and stress in the ocean lithosphere. *Journal of Geophysical Research*, **85**: 6403-6418.

Lewis AR, Marchant DR, Ashworth AC, Hemming SR, Machlus ML. 2007. Major middle Miocene global climate change: Evidence from East Antarctica and the Transantarctic Mountains. *Geological Society of America Bulletin*, **119**(11-12): 1449-1461.

Liu Z, Pagani M, Zinniker D, DeConto R, Huber M, Brinkhuis H, Shah SR, Leckie RM, Pearson A. 2009. Global cooling during the Eocene-Oligocene climate transition. *Science*, **323**(1187-1190).

Lythe M, Vaughan DG, Consortium B. 2001. BEDMAP: a new ice thickness and subglacial topographic model of Antarctica. *Journal of Geophysical Research*, **106**: 11335-11352.

MacGregor KR, Anderson RS, Anderson SP, Waddington ED. 2000. Numerical simulations of glacial-valley longitudinal profile evolution. *Geology*, **28**(11): 1031-1034.

Mackintosh A, White D, Fink D, Gore DB, Pickard J, Fanning PC. 2007. Exposure ages from mountain dipsticks in Mac. Robertson Land, East Antarctica, indicate little change in ice-sheet thickness since the Last Glacial Maximum. *Geology*, **35**(6): 551-554.

Marchant DR, Denton GH, Bockheim JG, Wilson SC, Kerr AR. 1994. Quaternary changes in level of the upper Taylor Glacier, Antarctica - implications for paleoclimate and East Antarctic ice-sheet dynamics. *Boreas*, **23**(1): 29-43.

Marchant DR, Denton GH, Swisher CC, III. 1993. Miocene-Pliocene-Pleistocene glacial history of Arena Valley, Quartermain Mountains, Antarctica. *Geografiska Annaler*, **75A**: 269-302.

Marchant DR, Denton GH, Swisher CC, Potter N. 1996. Late Cenozoic Antarctic paleoclimate reconstructed from volcanic ashes in the Dry Valleys region of southern Victoria Land. *Geological Society of America Bulletin*, **108**(2): 181-194.

Matthews RK, Poore RZ. 1980. Tertiary $\delta^{18}O$ record and glacio-eustatic sea-level fluctuations.

McCulloch RD, Sugden DE, Clapperton CM, Bentley MJ, Purves RS, Hulton NRJ. 2000. Climatic inferences from glacial and palaeoecological evidence at the last glacial termination, southern South America. *Journal of Quaternary Science*, **15**(4): 409-417.

Mildenhall DC. 1989. Terrestrial Palynology. In: Barrett PJ (Ed), *Antarctic Cenozoic History from the CIROS-1 Drillhole, McMurdo Sound. DSIR Bulletin 245*, pp. 119-127.

Miller GH, Fairbanks RG, Mountain GS. 1987. Tertiary oxygen isotope sysnthesis, sea-level history, and continental margin erosion. *Paleoceanography*, **2**: 1-19.

Miller KG, Wright JD, Browning JV. 2005. Visions of ice sheets in a greenhouse world. *Marine Geology*, **217**: 215-231.

Miller KG, Wright JD, Katz ME, Browning JV, Cramer BS, Wade BS, Mizintseva SF. 2008. A view of Antarctic ice-sheet evolution from sea-level and deep-sea isotope changes during the Late Cretaceous-Cenozoic. In: Cooper AK et al. (Eds), *Antarctica: A Keystone in a Changing World - Proceedings of the 10th International Symposium on Antarctic Earth Sciences.* The National Academies Press, Washington D.C., pp. 55-70.

Naish TR, Woolfe KJ, Barrett PJ, Wilson GS, Atkins C, Bohaty SM, Bucker CJ, Claps M, Davey FJ, Dunbar GB, Dunn AG, Fielding CR, Florindo F, Hannah MJ, Harwood DM, Henrys SA, Krissek LA, Lavelle M, van der Meer J, McIntosh WC, Niessen F, Passchier S, Powell RD, Roberts AP, Sagnotti L, Scherer RP, Strong CP, Talarico F, Verosub KL, Villa G, Watkins DK, Webb PN, Wonik T. 2001. Orbitally induced oscillations in the East Antarctic ice sheet at the Oligocene/Miocene boundary. *Nature*, **413**(6857): 719-723.

Naslund JO. 2001. Landscape development in western and central Dronning Maud Land, East Antarctica. *Antarctic Science*, **13**(3): 302-311.

O'Brien PE, Cooper AK, Richter C, al. e. 2001. Leg 188 summary: Prydz Bay-Cooperation Sea, Antarctica. *Proceedings of the Ocean Drilling Program.*, **Initial Reports 188**: 1-65.

Oerlemans J. 1984. Numerical experiments on large-scale glacial erosion. *Zeitschrift fur Gletscherkunde und Glazialgeologie*, **20**: 107-126.

Pagani M, Zachos JC, Freeman KH, Tipple B, Bohaty S. 2005. Marked decline in atmospheric carbon dioxide concentrations during the Paleogene. *Science*, **309**(5734): 600-603.

Paterson WSB. 1994. The physics of glaciers. 3rd edition, *The physics of glaciers. 3rd edition*. Pergamon, pp. 480.

Pearson PN, Palmer MR. 2000. Atmospheric carbon dioxide concentrations over the past 60 million years. *Nature*, **406**: 695-699.

Phillips WM, Hall AM, Mottram R, Fifield LK, Sugden D. 2006. Cosmogenic [10]Be and [26]Al exposure ages of tors and erratics, Cairngorm Mountains, Scotland: Timescales for the development of a classic landscape of selective linear glacial erosion. *Geomorphology*, **73**: 222-245.

Prebble JG, Raine JI, Barrett PJ, Hannah MJ. 2006. Vegetation and climate from two Oligocene glacioeustatic sedimentary cycles (31 and 24 Ma) cored by the Cape Roberts Project, Victoria Land Basin, Antarctica. *Palaeogeography, Palaeoclimatology, Palaeoecology*, **231**(1-2): 41-57.

Raine JI, Askin RA. 2001. Terrestrial palynology of Cape Roberts drillhole CRP-3, Victoria Land Basin, Antarctica. *Terra Antarctica*, **8**(389-400).

Reeh N. 1991. Parameterization of melt rate and surface temperature on the Greenland ice sheet. *Polarforschung*, **59**(3): 113-128.

Rippin DM, Bamber JL, Siegert MJ, Vaughan DG, Corr HFJ. 2004. The role of ice thickness and bed properties on the dynamics of the enhanced-flow tributaries of Bailey Ice Stream and Slessor Glacier, East Antarctica, *Annals of Glaciology, Vol 39, 2005*. Annals of Glaciology, pp. 366-372.

Rocchi S, LeMasurier WE, Di Vincenzo G. 2006. Oligocene to Holocene erosion and glacial history in Marie Byrd Land, West Antarctica, inferred from exhumation of the Dorrel Rock intrusive complex and from volcano morphologies. *Geological Society of America Bulletin*, **118**(7-8): 991-1005.

Rutt IC, Hagdorn M, Hulton NRJ, Payne AJ. 2009. The 'Glimmer' community ice sheet model. *Journal of Geophysical Research*, **114**: F02004.

Shevenell AE, Kennett JP, Lea DW. 2004. Middle Miocene Southern Ocean cooling and Antarctic cryosphere expansion. *Science*, **305**(5691): 1766-1770.

Siegert MJ, Taylor J, Payne AJ. 2005. Spectral roughness of subglacial topography and implications for former ice-sheet dynamics in East Antarctica. *Global and Planetary Change*, **45**(1-3): 249-263.

Stagg HMJ. 1985. The structure of Prydz Bay and MacRobertson Shelf, East Antarctica. *Tectonophysics*, **114**: 315-340.

Stern TA, Baxter AK, Barrett PJ. 2005. Isostatic rebound due to glacial erosion within the Transantarctic Mountains. *Geology*, **33**(3): 221.

Stroeven AP, Fabel D, Harbor J, Hättestrand C, Kleman J. 2002. Quantifying the erosional impact of the Fennoscandian ice sheet in the Torneträsk-Narvik corridor, northern Sweden, based on cosmogenic radionuclide data. *Geografiska Annaler, Series A: Physical Geography*, **84**(3-4): 275-287.

Stumpf AJ, Broster BE, Levson VM. 2000. Multiphase flow of the late Wisconsinan Cordilleran ice sheet in western Canada. *Geological Society of America Bulletin*, **112**(12): 1850-1863.

Sugden D, Denton G. 2004. Cenozoic landscape evolution of the Convoy Range to Mackay Glacier area, Transantartic Mountains: Onshore to offshore synthesis. *Bulletin of the Geological Society of America*, **116**(7-8): 840-857.

Sugden DE. 1978. Glacial erosion by the Laurentide ice sheet. *Journal of Glaciology*, **20**(83): 367-391.

Sugden DE, Balco G, Cowdery SG, Stone JO, Sass Iii LC. 2005. Selective glacial erosion and weathering zones in the coastal mountains of Marie Byrd Land, Antarctica. *Geomorphology*, **67**(3-4): 317-334.

Sugden DE, John BS. 1976. *Glaciers and Landscape*. Edward Arnold, 376 pp.

Sugden DE, Wilch TI, McIntosh WC, Marchant DR, Rutford RH, Summerfield MA, Denton GH. 1999. Landscape development in the Royal Society Range, southern Victoria Land, Antartica: Stability since the mid-Miocene. *Geomorphology*, **28**(3-4): 181-200.

Taylor J, O'Brien PE, Cooper AK, Leitchenkov G, Siegert MJ, Payne AJ, Hambrey MJ. 2004. Topographic controls on post-Oligocene changes in ice-sheet dynamics, Prydz Bay region, East Antarctica. *Geology*, **32**(3): 197-200.

Tomkin JH. 2003. Erosional feedbacks and the oscillation of ice masses. *Journal of Geophysical Research B: Solid Earth*, **108**(B10): ETG 12-1 - ETG 12-12.

Tomkin JH, Braun J. 2002. The influence of alpine glaciation on the relief of tectonically active mountain belts. *American Journal of Science*, **302**(3): 169-190.

Vaughan DG, Bamber JL, Giovinetto M, Russell J, Cooper APR. 1999. Reassessment of net surface mass balance in Antarctica. *Journal of Climate*, **12**(4): 933-946.

Webb PN. 1994. Palaeo-drainage systems of East Antarctica and sediment supply systems to West Antarctic Rift System basins. *Terra Antarctica*, **1**: 457-461.

Wilson DS, Luyendyk BP. 2009. West Antarctic paleotopography estimated at the Eocene-Oligocene climate transition. *Geophysical Research Letters*, **36**: L16302.

Zachos JC, Kump LR. 2005. Carbon cycle feedbacks and the initiation of Antarctic glaciation in the earliest Oligocene. *Global and Planetary Change*, **47**: 51-66.
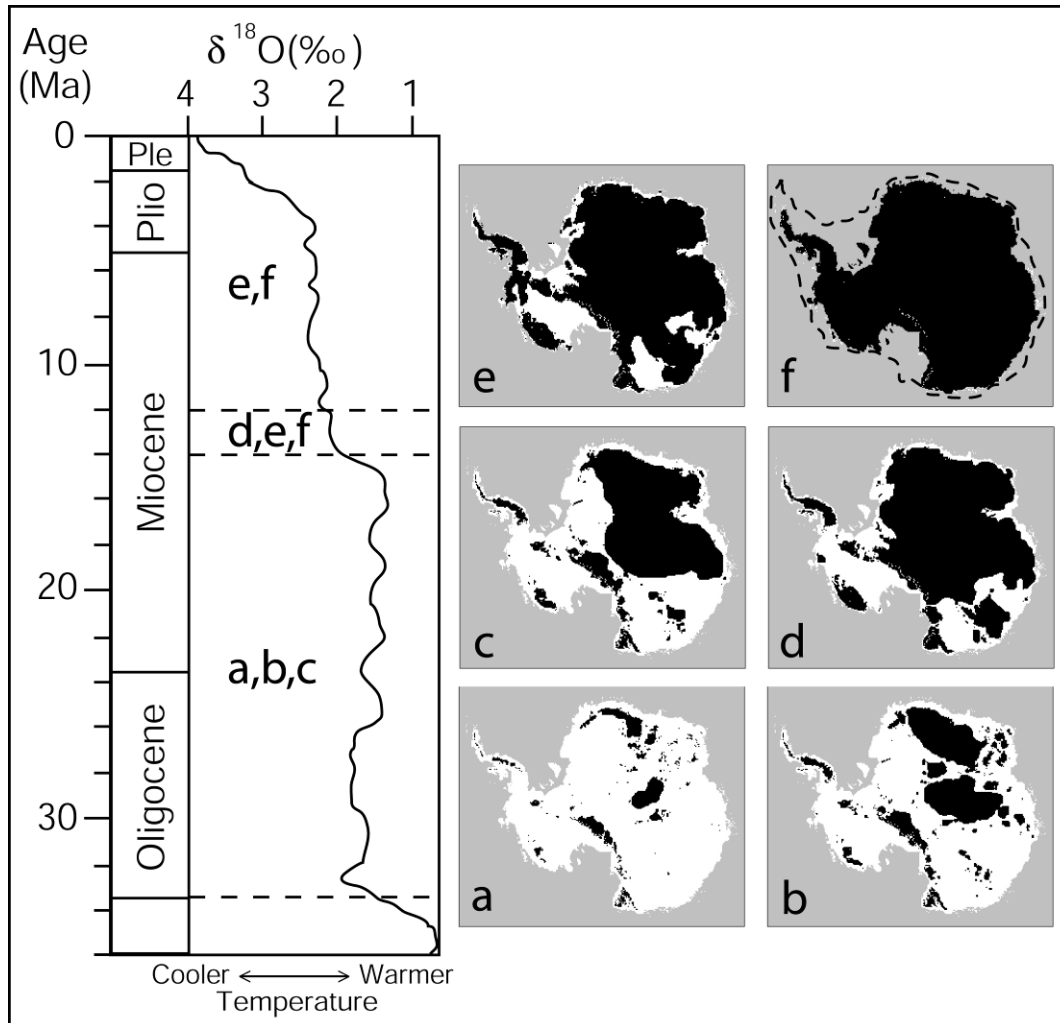
Figures and Tables:

Figure 1: Global deep-sea oxygen isotope curve indicating glacial intensity over the various stages of Antarctic glaciation. The record is smoothed using a Gaussian function and therefore shows shifts on million year timescales. From Miller et al., (1987; 2005). Labels e-f (bounded by dashed lines representing timing of known glacial extent changes) correspond to schematics a-f which show the range of ice mass extents (black) which are used to understand average basal conditions potentially associated with each time period. White areas show parts of the landscape that may be modified by glacial erosion, and that we therefore investigate in the course of this paper. The dashed line surrounding scenario f illustrates maximum ice sheet extension to the continental shelf edge (e.g. 14 Ma), and is not modelled here.
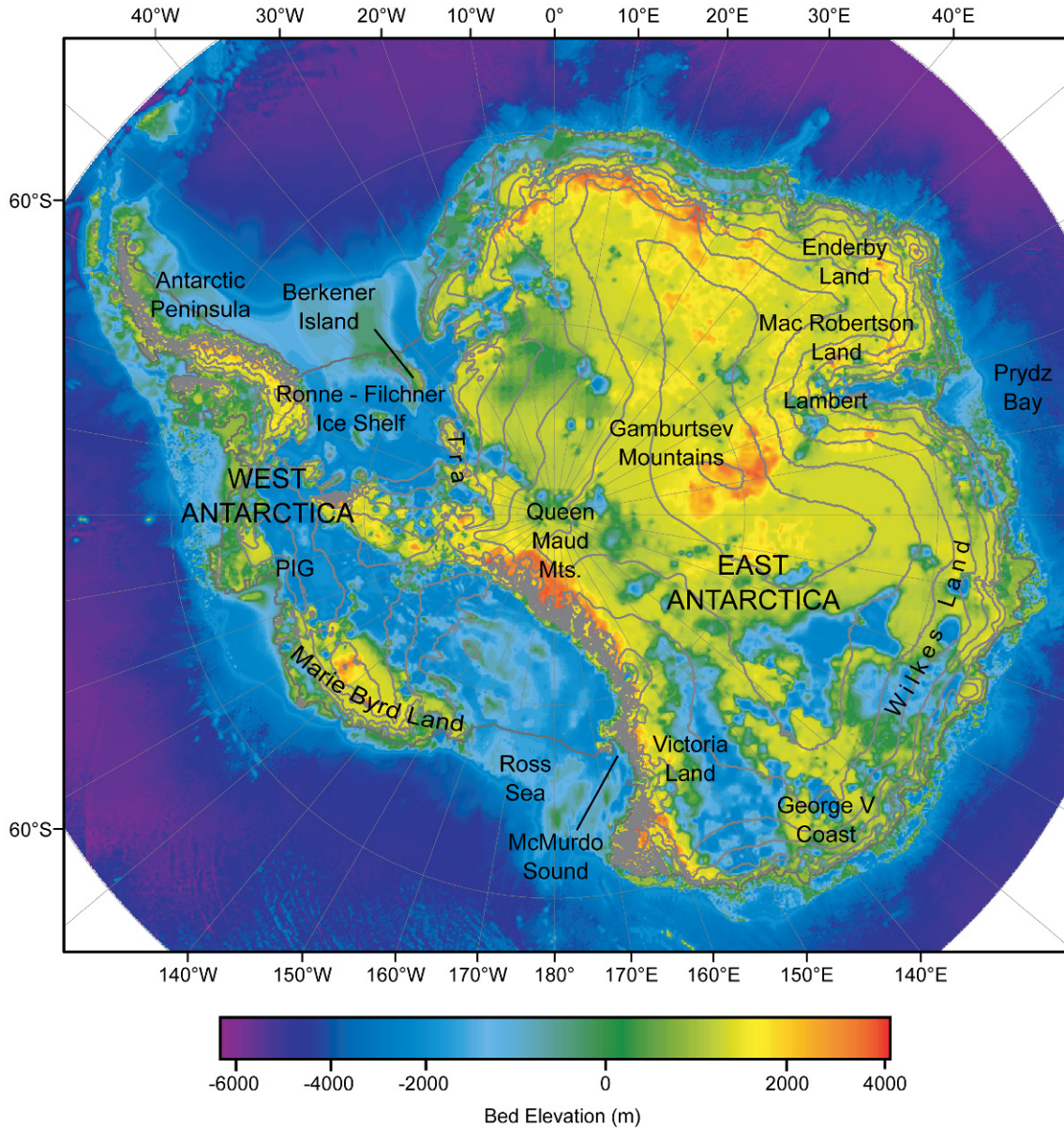
Figure 2: Present-day subglacial landscape, ice surface elevation (500 m contour intervals). Data from BEDMAP (Lythe et al., 2001).

Figure 3: Glacial landforms resulting from distinctive basal thermal regimes. Formerly glaciated landscapes in the northern hemisphere provide insight into the likely landforms at the bed of the present day Antarctic Ice Sheet: (A) The summit plateau of Ben Avon in the Cairngorm Mountains, Scotland. The plateau and its granite tors survived beneath cold-based ice during the Pleistocene glaciations of Scotland (Phillips et al., 2006); (B) A landscape of areal scouring at the foot of Suilven in the NW Highlands of Scotland (courtesy British Geological Survey, ref: P000958). The scouring is the result of erosion beneath warm-based ice (Gordon, 1981); (C) Selective trough incision by outlet glaciers with adjacent cold-based ice on the adjacent plateaus, Blosseville Coast, East Greenland (courtesy Geodetic Institute, Denmark).
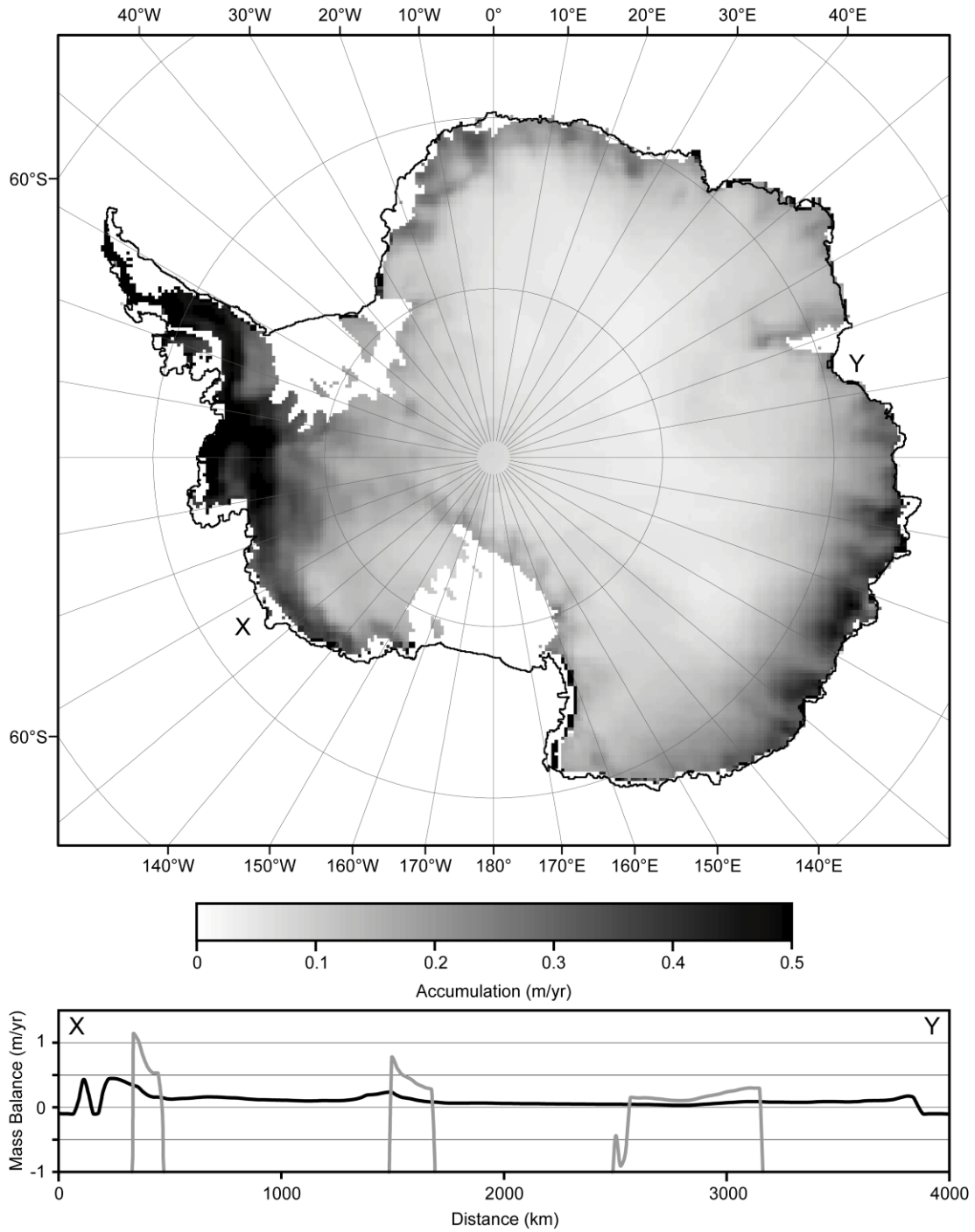
Figure 4: Present-day accumulation in Antarctica. Profiles X-Y show mass balance for present-day (black) and under a warmer Patagonian style climate (grey). Under a Patagonian regime, there are zones of increased accumulation at high altitudes and high ablation rates in the continental lowlands. After Vaughan (1999) and Jamieson and Sugden (2008).
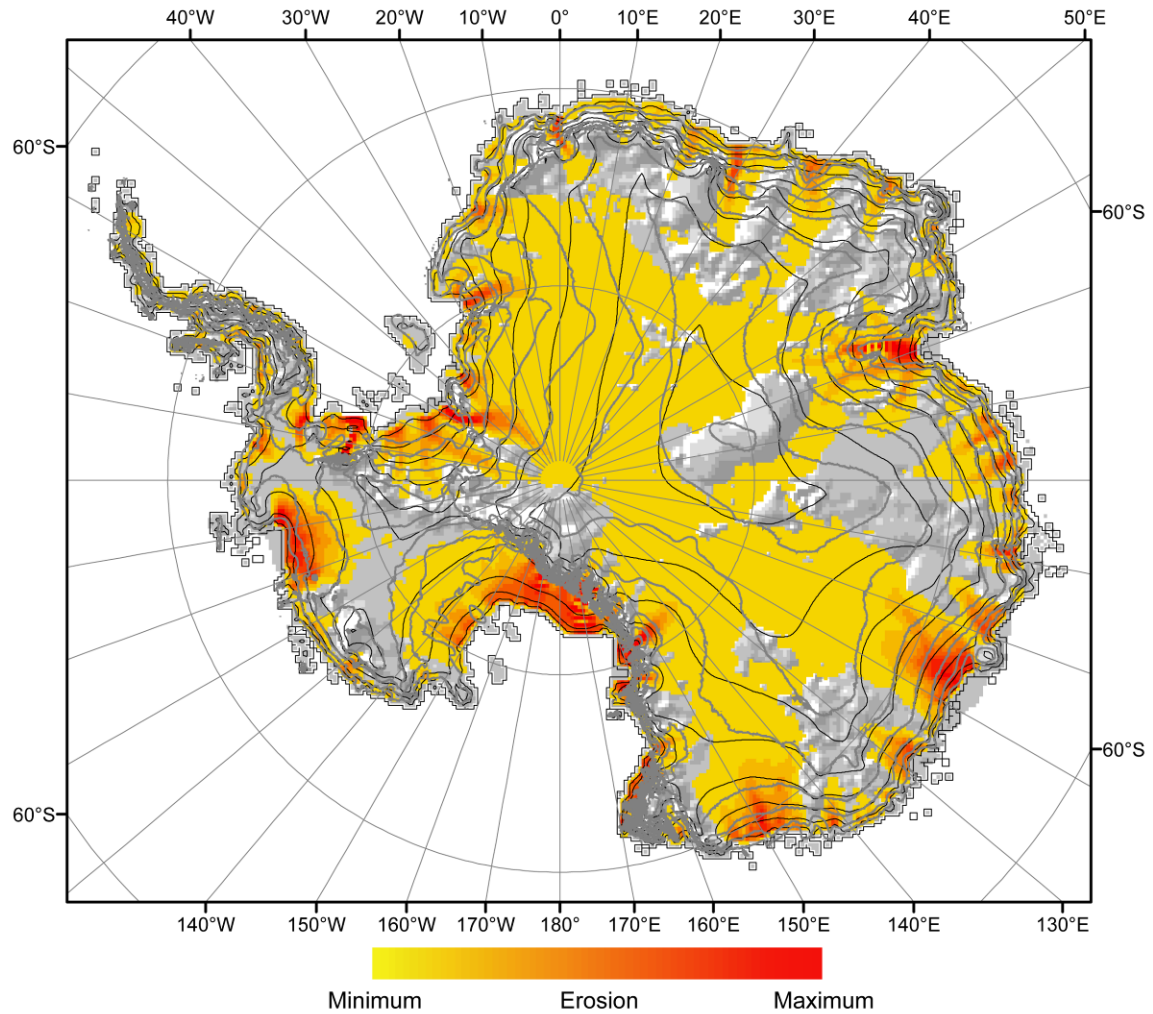
Figure 5: Comparison between modelled and present-day ice-sheets, showing present-day ice surface (grey contours), modelled present-day ice surface (black contours) and modelled zones of erosion based on basal sliding conditions. Contours are at 500 m intervals. Areas with no colour indicate cold-based ice at the present-day.
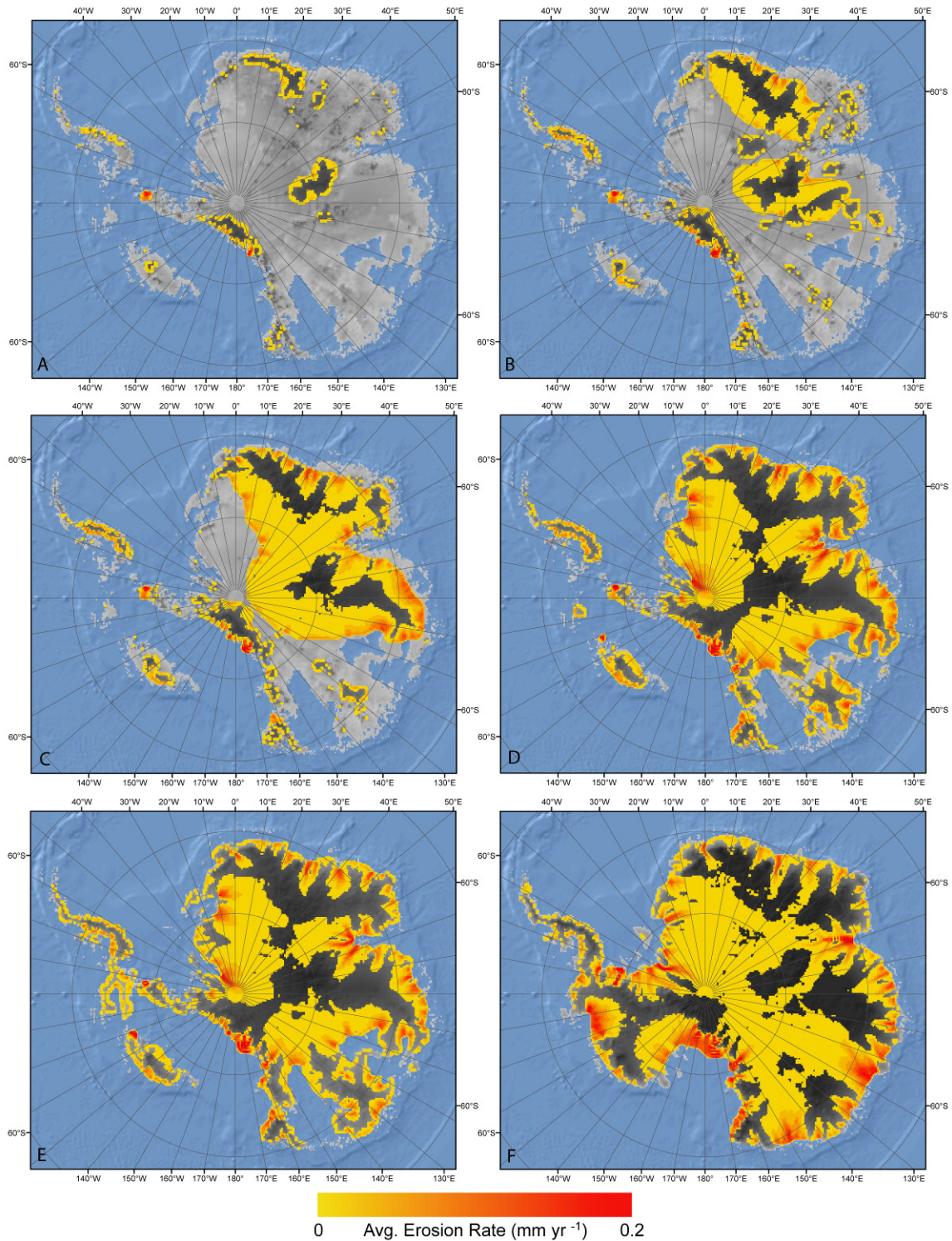
Figure 6: Modelled erosion rates at six stages of ice-sheet evolution. The corresponding mean annual air temperatures at sea level from A-F are: 6.5 °C, 2.4 °C, 0.8 °C, -3.9 °C, -6.6 °C and -15 °C. The light greyscale shading shows land surface above sea level, dark shading indicates cold-based ice and blue represents sea level.
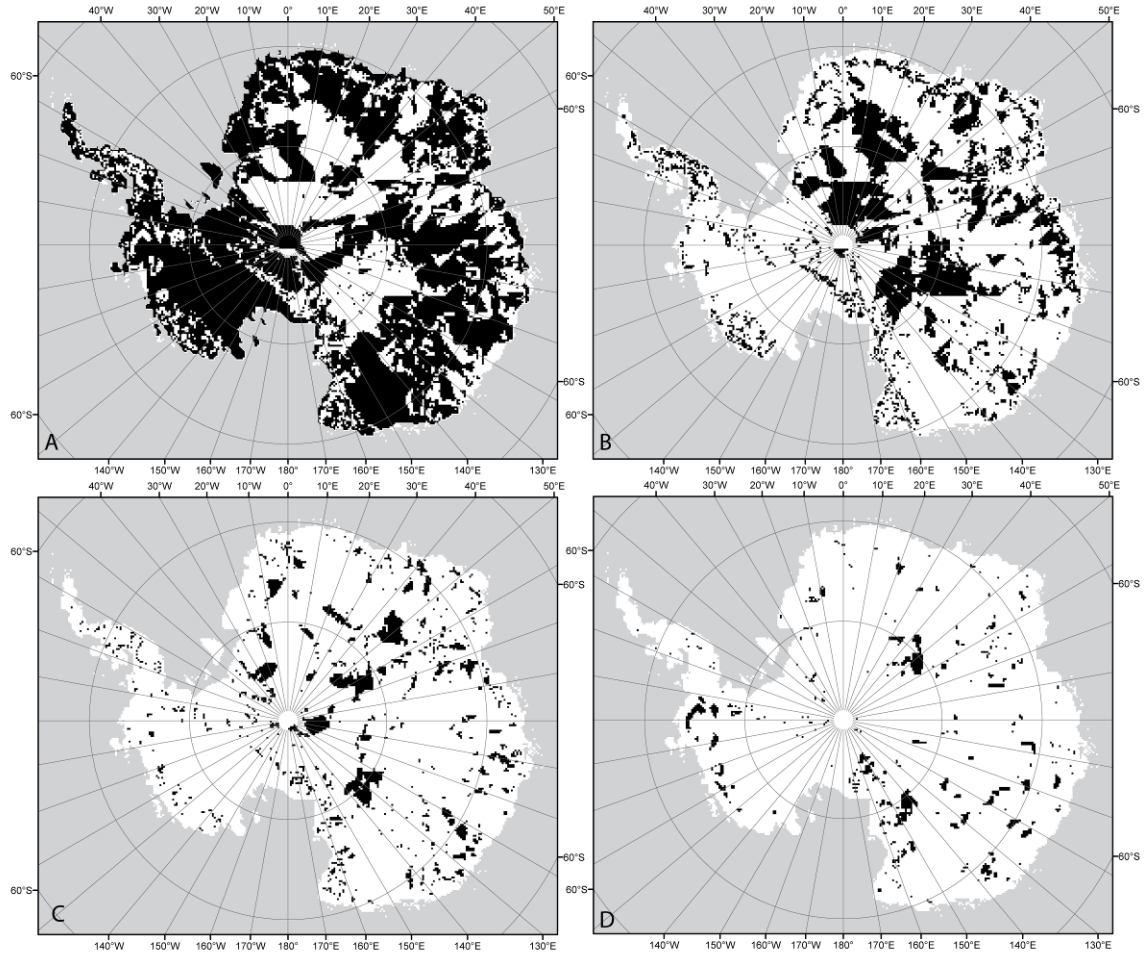
Figure 7: Maximum changes in modelled basal ice flow direction calculated using the snapshots of glacial extent (Fig. 6). Basal flow direction changes by: (A) less than 10 degrees; (B) 10-45 degrees; (C) 45-90 degrees and (D) 90-180 degrees.
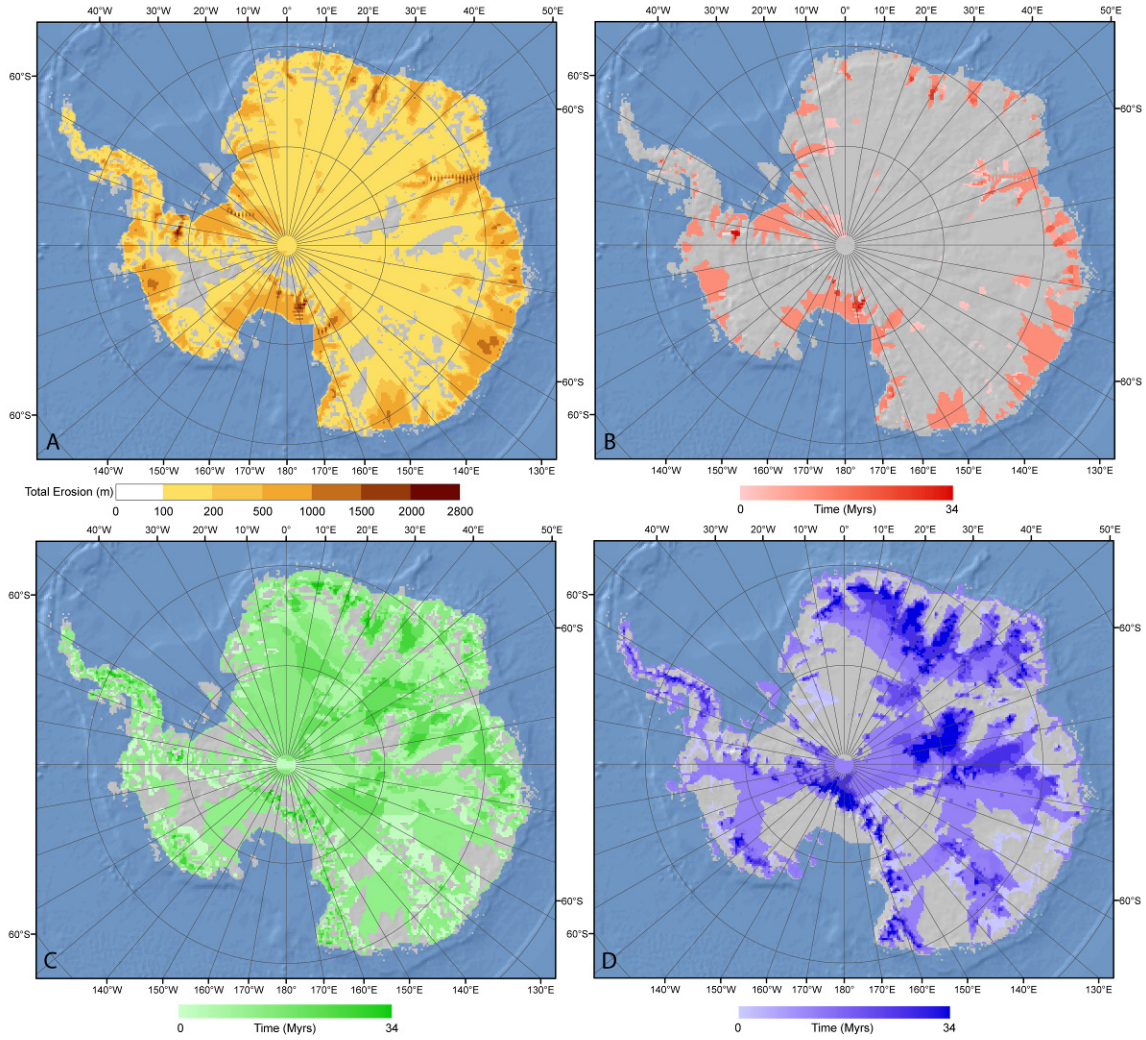
Figure 8: Time-integrated analysis of modelled total erosion and the duration of particular erosion regimes across Antarctica. (A) Total depths of erosion based on integration of erosion rates through time. The maximum value of ca. 2800 m relates to a modelled maximum average erosion rate of 0.2 mm yr^{-1}. Maps also indicate the length of time parts of Antarctica experienced: (B) selective erosion; (C) areal scouring; (D) cold-based ice.
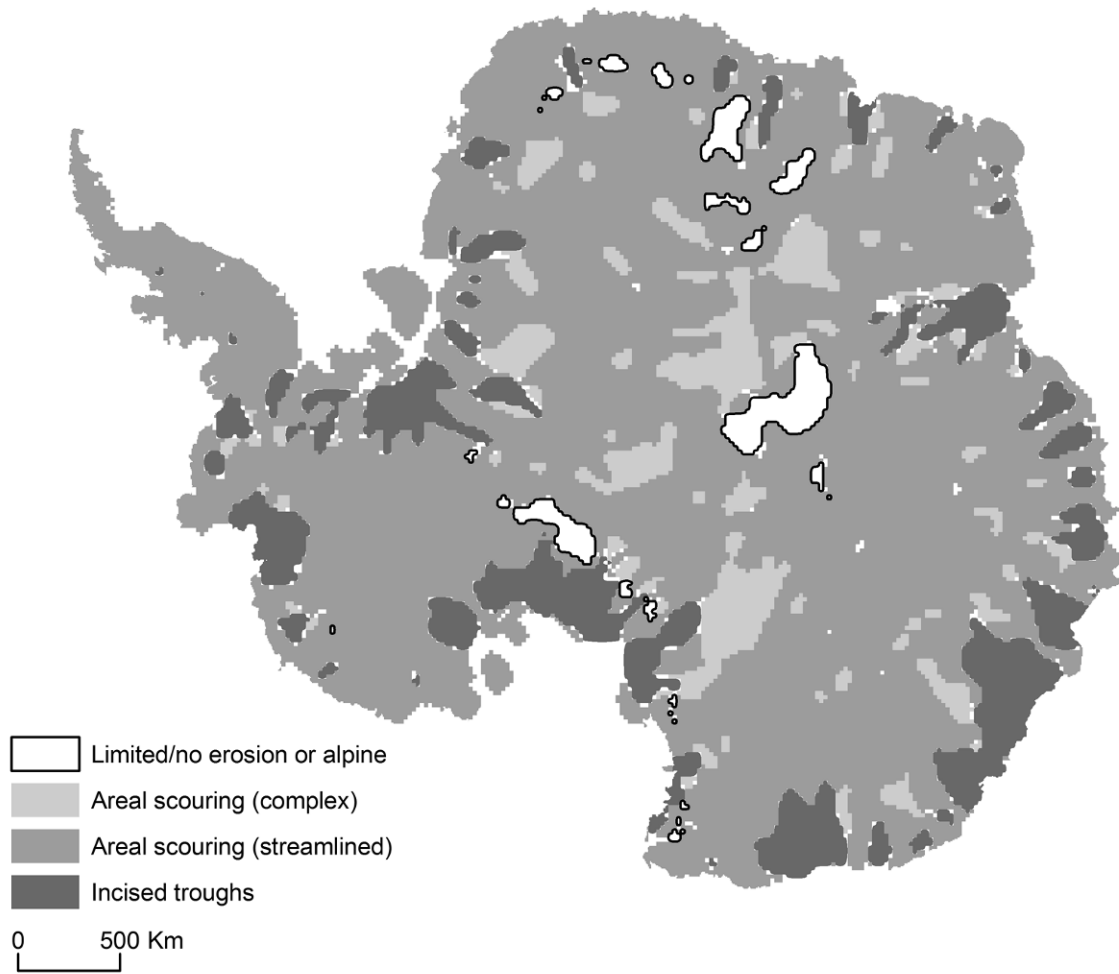
Figure 9: Map of the geomorphological nature of the contemporary subglacial landscape of Antarctica predicted by modelling. The map is generalised for clarity by using a moving window approach that assumes any cells inside a 60 km search radius from each location are the same as the majority of cells within that radius.

Time	Details	Ice-sheet Scale
34-14 Ma	Ice-sheets oscillate on similar scales to northern hemisphere Pleistocene ice-sheets (Naish et al., 2001; Pekar and DeConto, 2006). This is analogous to fluctuations between growth scales 1-3 in our model and we classify this by assigning 6.66 Myrs of time to each of these three states (a total of 20 Myrs).	(Fig. 6a-c)
14-13.6 Ma	Step cooling drives ice expansion to its maximum offshore extent creating a continental polar ice-sheet (Anderson, 1999; Denton et al., 1993; Holbourn et al., 2005; Marchant et al., 1996). We assign 0.2 Myrs to each model step.	(Fig. 6d-f)
13.6-0 Ma	East Antarctic Ice Sheet and West Antarctic Ice Sheet are confined to the continent with relatively minor fluctuations driven by sea-level change (Denton and Hughes, 1986; Denton et al., 1993; Marchant et al., 1996). This 13.6 Myrs of Antarctic glacial history is captured in our model by the final step.	(Fig. 6e-f)

Table 1: Division of time applied to each scale of modelled ice-sheet in order to calculate the nature of erosion across Antarctica since the Oligocene (section 2.3).